EUROPEAN LABORATORY FOR PARTICLE PHYSICS (CERN)

CERN-PPE/93-52
15 March 1993

Search for contact interactions in the reactions $e^+e^- \to \ell^+\ell^-$ and $e^+e^- \to \gamma\gamma$

The ALEPH Collaboration

Abstract

Contact interactions are searched for using the differential cross sections for the reactions $e^+e^- \to e^+e^-$, $e^+e^- \to \mu^+\mu^-$, $e^+e^- \to \tau^+\tau^-$ and $e^+e^- \to \gamma\gamma$ measured at 12 energies around the Z peak and corresponding to about 20 pb^{-1} of cumulated luminosity. Four-fermion contact term models assuming various chiralities of lepton currents are fitted to the lepton data and lower limits on the energy scale Λ of such terms are set at 95 % c.l. The limits vary in the range 0.9–4.7 TeV, depending on the model and on the lepton flavour. The $ee\gamma\gamma$ contact terms are searched for assuming various chiralities. Limits on the energy scale Λ between 79 and 130 GeV are extracted from the data. The results are compared and combined with those reported at lower energies.

Submitted to *Zeitschrift für Physik C*

The ALEPH Collaboration

D. Buskulic, D. Decamp, C. Goy, J.-P. Lees, M.-N. Minard, B. Mours, B. Pietrzyk

Laboratoire de Physique des Particules (LAPP), IN^{2}P^3-CNRS, 74019 Annecy-le-Vieux Cedex, France

R. Alemany, F. Ariztizabal, P. Comas, J.M. Crespo, M. Delfino, E. Fernandez, M. Fernandez-Bosman, V. Gaitan, Ll. Garrido, T. Mattison, A. Pacheco, C. Padilla, A. Pascual

Institut de Fisica d'Altes Energies, Universitat Autonoma de Barcelona, 08193 Bellaterra (Barcelona), Spain[7]

D. Creanza, M. de Palma, A. Farilla, G. Iaselli, G. Maggi, M. Maggi, S. Natali, S. Nuzzo, M. Quattromini, A. Ranieri, G. Raso, F. Romano, F. Ruggieri, G. Selvaggi, L. Silvestris, P. Tempesta, G. Zito

INFN Sezione di Bari e Dipartimento di Fisica dell' Università, 70126 Bari, Italy

Y. Chai, H. Hu, D. Huang, X. Huang, J. Lin, T. Wang, Y. Xie, D. Xu, R. Xu, J. Zhang, L. Zhang, W. Zhao

Institute of High-Energy Physics, Academia Sinica, Beijing, The People's Republic of China[8]

L.A.T. Bauerdick,[23] E. Blucher, G. Bonvicini, J. Boudreau, D. Casper, H. Drevermann, R.W. Forty, G. Ganis, C. Gay, R. Hagelberg, J. Harvey, S. Haywood, J. Hilgart, R. Jacobsen, B. Jost, J. Knobloch, I. Lehraus, T. Lohse,[29] A. Lusiani, M. Martinez, P. Mato, H. Meinhard, A. Minten, A. Miotto, R. Miquel, H.-G. Moser, P. Palazzi, J.A. Perlas, J.-F. Pusztaszeri, F. Ranjard, G. Redlinger,[24] L. Rolandi, J. Rothberg,[2] T. Ruan, M. Saich, D. Schlatter, M. Schmelling, F. Sefkow, W. Tejessy, H. Wachsmuth, W. Wiedenmann, T. Wildish, W. Witzeling, J. Wotschack

European Laboratory for Particle Physics (CERN), 1211 Geneva 23, Switzerland

Z. Ajaltouni, F. Badaud, M. Bardadin-Otwinowska, R. El Fellous, A. Falvard, P. Gay, C. Guicheney, P. Henrard, J. Jousset, B. Michel, J-C. Montret, D. Pallin, P. Perret, F. Podlyski, J. Proriol, F. Prulhière, F. Saadi

Laboratoire de Physique Corpusculaire, Université Blaise Pascal, IN^{2}P^3-CNRS, Clermont-Ferrand, 63177 Aubière, France

T. Fearnley, J.D. Hansen, J.R. Hansen,[1] P.H. Hansen, R. Møllerud, B.S. Nilsson[1]

Niels Bohr Institute, 2100 Copenhagen, Denmark[9]

I. Efthymiopoulos, A. Kyriakis, E. Simopoulou, A. Vayaki, K. Zachariadou

Nuclear Research Center Demokritos (NRCD), Athens, Greece

J. Badier, A. Blondel, G. Bonneaud, J.C. Brient, G. Fouque, S. Orteu, A. Rougé, M. Rumpf, R. Tanaka, M. Verderi, H. Videau

Laboratoire de Physique Nucléaire et des Hautes Energies, Ecole Polytechnique, IN^{2}P^3-CNRS, 91128 Palaiseau Cedex, France

D.J. Candlin, M.I. Parsons, E. Veitch

Department of Physics, University of Edinburgh, Edinburgh EH9 3JZ, United Kingdom[10]

L. Moneta, G. Parrini

Dipartimento di Fisica, Università di Firenze, INFN Sezione di Firenze, 50125 Firenze, Italy

M. Corden, C. Georgiopoulos, M. Ikeda, J. Lannutti, D. Levinthal,[15] M. Mermikides†, L. Sawyer, S. Wasserbaech

Supercomputer Computations Research Institute and Dept. of Physics, Florida State University, Tallahassee, FL 32306, USA [12,13,14]

A. Antonelli, R. Baldini, G. Bencivenni, G. Bologna,[4] F. Bossi, P. Campana, G. Capon, F. Cerutti, V. Chiarella, B. D'Ettorre-Piazzoli,[25] G. Felici, P. Laurelli, G. Mannocchi,[5] F. Murtas, G.P. Murtas, L. Passalacqua, M. Pepe-Altarelli, P. Picchi[4]

Laboratori Nazionali dell'INFN (LNF-INFN), 00044 Frascati, Italy

P. Colrain, I. ten Have, J.G. Lynch, W. Maitland, W.T. Morton, C. Raine, P. Reeves, J.M. Scarr, K. Smith, M.G. Smith, A.S. Thompson, R.M. Turnbull

Department of Physics and Astronomy, University of Glasgow, Glasgow G12 8QQ,United Kingdom[10]

B. Brandl, O. Braun, C. Geweniger, P. Hanke, V. Hepp, E.E. Kluge, Y. Maumary, A. Putzer, B. Rensch, A. Stahl, K. Tittel, M. Wunsch

Institut für Hochenergiephysik, Universität Heidelberg, 6900 Heidelberg, Fed. Rep. of Germany[16]

R. Beuselinck, D.M. Binnie, W. Cameron, M. Cattaneo, D.J. Colling, P.J. Dornan, A.M. Greene, J.F. Hassard, N.M. Lieske,[31] A. Moutoussi, J. Nash, S. Patton, D.G. Payne, M.J. Phillips, G. San Martin, J.K. Sedgbeer, I.R. Tomalin, A.G. Wright

Department of Physics, Imperial College, London SW7 2BZ, United Kingdom[10]

P. Girtler, E. Kneringer, D. Kuhn, G. Rudolph

Institut für Experimentalphysik, Universität Innsbruck, 6020 Innsbruck, Austria[18]

C.K. Bowdery, T.J. Brodbeck, A.J. Finch, F. Foster, G. Hughes, D. Jackson, N.R. Keemer, M. Nuttall, A. Patel, T. Sloan, S.W. Snow, E.P. Whelan

Department of Physics, University of Lancaster, Lancaster LA1 4YB, United Kingdom[10]

K. Kleinknecht, J. Raab, B. Renk, H.-G. Sander, H. Schmidt, F. Steeg, S.M. Walther, R. Wanke, B. Wolf

Institut für Physik, Universität Mainz, 6500 Mainz, Fed. Rep. of Germany[16]

A.M. Bencheikh, C. Benchouk, A. Bonissent, J. Carr, P. Coyle, J. Drinkard,[3] F. Etienne, D. Nicod, S. Papalexiou, P. Payre, L. Roos, D. Rousseau, P. Schwemling, M. Talby

Centre de Physique des Particules, Faculté des Sciences de Luminy, IN^{2}P^3-CNRS, 13288 Marseille, France

S. Adlung, R. Assmann, C. Bauer, W. Blum, D. Brown, P. Cattaneo,[28] B. Dehning, H. Dietl, F. Dydak,[22] M. Frank, A.W. Halley, J. Lauber, G. Lütjens, G. Lutz, W. Männer, R. Richter, H. Rotscheidt, J. Schröder, A.S. Schwarz, R. Settles, H. Seywerd, U. Stierlin, U. Stiegler, R. St. Denis, G. Wolf

Max-Planck-Institut für Physik, Werner-Heisenberg-Institut, 8000 München, Fed. Rep. of Germany[16]

J. Boucrot,[1] O. Callot, A. Cordier, M. Davier, L. Duflot, J.-F. Grivaz, Ph. Heusse, D.E. Jaffe, P. Janot, D.W. Kim,[19] F. Le Diberder, J. Lefrançois, A.-M. Lutz, M.-H. Schune, J.-J. Veillet, I. Videau, Z. Zhang,

Laboratoire de l'Accélérateur Linéaire, Université de Paris-Sud, IN^{2}P^3-CNRS, 91405 Orsay Cedex, France

D. Abbaneo, G. Bagliesi, G. Batignani, L. Bosisio, U. Bottigli, C. Bozzi, G. Calderini, M. Carpinelli, M.A. Ciocci, R. Dell'Orso, I. Ferrante, F. Fidecaro, L. Foà, E. Focardi, F. Forti, A. Giassi, M.A. Giorgi, A. Gregorio, F. Ligabue, E.B. Mannelli, P.S. Marrocchesi, A. Messineo, F. Palla, G. Rizzo, G. Sanguinetti, P. Spagnolo, J. Steinberger, R. Tenchini, G. Tonelli, G. Triggiani, C. Vannini, A. Venturi, P.G. Verdini, J. Walsh

Dipartimento di Fisica dell'Università, INFN Sezione di Pisa, e Scuola Normale Superiore, 56010 Pisa, Italy

A.P. Betteridge, J.M. Carter, M.G. Green, P.V. March, Ll.M. Mir, T. Medcalf, I.S. Quazi, J.A. Strong, L.R. West

Department of Physics, Royal Holloway & Bedford New College, University of London, Surrey TW20 OEX, United Kingdom[10]

D.R. Botterill, R.W. Clifft, T.R. Edgecock, M. Edwards, S.M. Fisher, T.J. Jones, P.R. Norton, D.P. Salmon, J.C. Thompson

Particle Physics Dept., Rutherford Appleton Laboratory, Chilton, Didcot, Oxon OX11 OQX, United Kingdom[10]

B. Bloch-Devaux, P. Colas, H. Duarte, W. Kozanecki, E. Lançon, M.C. Lemaire, E. Locci, P. Perez, F. Perrier, J. Rander, J.-F. Renardy, A. Rosowsky, A. Roussarie, J.-P. Schuller, J. Schwindling, D. Si Mohand, B. Vallage

Service de Physique des Particules, DAPNIA, CE-Saclay, 91191 Gif-sur-Yvette Cedex, France[17]

R.P. Johnson, A.M. Litke, G. Taylor, J. Wear

Institute for Particle Physics, University of California at Santa Cruz, Santa Cruz, CA 95064, USA[27]

J.G. Ashman, W. Babbage, C.N. Booth, C. Buttar, R.E. Carney, S. Cartwright, F. Combley, F. Hatfield, L.F. Thompson[1]

Department of Physics, University of Sheffield, Sheffield S3 7RH, United Kingdom[10]

E. Barberio, A. Böhrer, S. Brandt, G. Cowan, C. Grupen, G. Lutters, F. Rivera,[32] U. Schäfer, L. Smolik

Fachbereich Physik, Universität Siegen, 5900 Siegen, Fed. Rep. of Germany[16]

R. Della Marina, G. Giannini, B. Gobbo, F. Ragusa[21]

Dipartimento di Fisica, Università di Trieste e INFN Sezione di Trieste, 34127 Trieste, Italy

L. Bellantoni, W. Chen, D. Cinabro,[26] J.S. Conway,[30] D.F. Cowen,[20] Z. Feng, D.P.S. Ferguson, Y.S. Gao, J. Grahl, J.L. Harton, R.C. Jared,[6] B.W. LeClaire, C. Lishka, Y.B. Pan, J.R. Pater, Y. Saadi, M. Schmitt, V. Sharma, Z.H. Shi, A.M. Walsh, F.V. Weber, Sau Lan Wu, X. Wu, M. Zheng, G. Zobernig

Department of Physics, University of Wisconsin, Madison, WI 53706, USA[11]

---

†Deceased.

[1]Now at CERN, PPE Division, 1211 Geneva 23, Switzerland.

[2]Permanent address: University of Washington, Seattle, WA 98195, USA.

[3]Now at University of California, Irvine, CA 92717, USA.

[4]Also Istituto di Fisica Generale, Università di Torino, Torino, Italy.

[5]Also Istituto di Cosmo-Geofisica del C.N.R., Torino, Italy.

[6]Permanent address: LBL, Berkeley, CA 94720, USA.

[7]Supported by CICYT, Spain.

[8]Supported by the National Science Foundation of China.

[9]Supported by the Danish Natural Science Research Council.

[10]Supported by the UK Science and Engineering Research Council.

[11]Supported by the US Department of Energy, contract DE-AC02-76ER00881.

[12]Supported by the US Department of Energy, contract DE-FG05-87ER40319.

[13]Supported by the NSF, contract PHY-8451274.

[14]Supported by the US Department of Energy, contract DE-FC0S-85ER250000.

[15]Supported by SLOAN fellowship, contract BR 2703.

[16]Supported by the Bundesministerium für Forschung und Technologie, Fed. Rep. of Germany.

[17]Supported by the Direction des Sciences de la Matière, C.E.A.

[18]Supported by Fonds zur Förderung der wissenschaftlichen Forschung, Austria.

[19]Supported by the Korean Science and Engineering Foundation and Ministry of Education.

[20]Now at California Institute of Technology, Pasadena, CA 91125, USA.

[21]Now at Dipartimento di Fisica, Università di Milano, Milano, Italy.

[22]Also at CERN, PPE Division, 1211 Geneva 23, Switzerland.

[23]Now at DESY, Hamburg, Germany.

[24]Now at TRIUMF, Vancouver, B.C., Canada.

[25]Also at Università di Napoli, Dipartimento di Scienze Fisiche, Napoli, Italy.

[26]Now at Harvard University, Cambridge, MA 02138, U.S.A.

[27]Supported by the US Department of Energy, grant DE-FG03-92ER40689.

[28]Now at Università di Pavia, Pavia, Italy.

[29]Now at Max-Planck-Institut f. Kernphysik, Heidelberg, Germany.

[30]Now at Rutgers University, Piscataway, NJ 08854, USA.

[31]Now at Oxford University, Oxford OX1 3RH, U.K.

[32]Partially supported by Colciencias, Colombia.

1 Introduction

Precise measurements at LEP can be used to search for an indirect manifestation of new physics. The basic idea is that the standard model is a part of a more general theory characterized by an energy scale Λ. At energies well below Λ the observable consequences of the theory are reduced to a residual effective interaction called the contact term considered as a perturbation to the standard model. In the context of a possible substructure of quarks and leptons, contact terms may be interpreted as remnants of a constituent-binding interaction at the compositeness scale Λ. More generally, the formalism of contact terms is a useful parametrisation of possible deviations from the standard model; the deviations might have various dynamic origins such as a composite nature of the Z, new bosons, excited fermion exchange, anomalous couplings, etc.

In the contact interaction approach [1, 2, 3, 4, 5] the standard model Lagrangian remains unchanged but an effective Lagrangian due to a new interaction is added to it. The latter is built from the fields of presently known particles and is proportional to the lowest possible power of $1/\Lambda$ depending on the dimension of the fields involved. The fermion currents are required to be helicity conserving. This assumption is necessary for example in composite models in order to keep the masses of known particles much smaller than Λ. Various possible choices of the chiralities lead to different predictions for the angular distributions of the reactions where contact terms contribute.

Four-lepton contact terms are searched for in the reactions $e^+e^- \to e^+e^-$, $e^+e^- \to \mu^+\mu^-$, $e^+e^- \to \tau^+\tau^-$ and in the three reactions combined, assuming lepton universality. Two-photon, two-electron contact terms are studied in the reaction $e^+e^- \to \gamma\gamma$. The analysis makes use of the differential cross sections at several energies around the Z peak measured by ALEPH using the data sample of integrated luminosity 20.5 pb^{-1} collected in 1989-91. The ALEPH detector is described elsewhere [6].

2 Four-lepton contact terms

Four-lepton contact interactions are described, according to Eichten, Lane and Peskin [1], by an effective Lagrangian in the form:

$$\mathcal{L}_{eell} = k_{el}\frac{g^2}{2\Lambda^2}\left[\eta_{LL}\overline{\psi^e_L}\gamma_\mu\psi^e_L\overline{\psi^\ell_L}\gamma^\mu\psi^\ell_L + \eta_{RR}\overline{\psi^e_R}\gamma_\mu\psi^e_R\overline{\psi^\ell_R}\gamma^\mu\psi^\ell_R + \eta_{RL}\overline{\psi^e_R}\gamma_\mu\psi^e_R\overline{\psi^\ell_L}\gamma^\mu\psi^\ell_L + \eta_{LR}\overline{\psi^e_L}\gamma_\mu\psi^e_L\overline{\psi^\ell_R}\gamma^\mu\psi^\ell_R\right],$$

where k_{el} is a statistical factor equal to 1/2 for $\ell = e$ and to 1 otherwise. The fermion currents are flavour diagonal: four different currents can be constructed in the reaction $e^+e^- \to e^+e^-$ and only two for other lepton flavours. The interaction is proportional to Λ^{-2} since the product of the four fermion fields has the dimension of the 6-th power of energy. By convention, the Lagrangian is normalized to the effective strong coupling constant, $g^2/4\pi$ =1. The coefficients η_{ij}, $i,j = R,L$ indicate the chiralities of the fermion currents. A contact term model is defined by a set of

values of η_{LL}, η_{RR}, η_{RL}, η_{LR} and the corresponding Λ. The contact term amplitude is real and can be either positive or negative; with each sign a different Λ is associated. Alltogether 6×2 models listed in table 1 are studied.

Model	η_{LL}	η_{RR}	η_{RL}	η_{LR}
LL	± 1	0	0	0
RR	0	± 1	0	0
VV	± 1	± 1	± 1	± 1
AA	± 1	± 1	∓ 1	∓ 1
RL	0	0	± 1	0
LR	0	0	0	± 1

Table 1: Definition of the parameters of the four-fermion contact models.

2.1 Differential cross section

The lowest order diagrams for the reaction $e^+e^- \to \ell^+\ell^-$ are shown in fig.1.

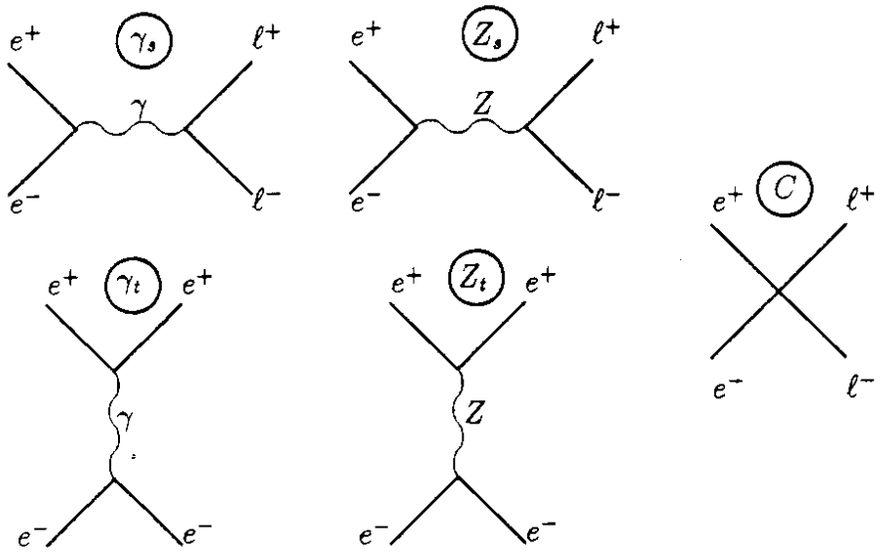

Figure 1: Lowest order diagrams contributing to the reaction $e^+e^- \to \ell^+\ell^-$.

The differential cross section can be written symbolically as

$$\frac{d\sigma}{d\Omega} \sim |\gamma_s + Z_s + \gamma_t + Z_t + C|^2$$

In the expansion of this expression the terms are:

$|\gamma_s + Z_s|^2$, standard model s-channel exchange amplitude squared,

$|C|^2$, contact term amplitude squared, proportional to $1/\Lambda^4$,

$2\,\Re e\,[(\gamma_s + Z_s)C]$, interference between the s-channel standard model amplitude and the contact term. This contribution is proportional to $1/\Lambda^2$ and therefore it is generally expected to be much larger than $|C|^2$. However very close to the Z peak the standard model amplitude is almost purely imaginary and consequently its interference with the real contact term is small.

Terms present only for the reaction $e^+e^- \to e^+e^-$ are:

$|\gamma_t+Z_t|^2+2\,\Re e\,[(\gamma_t + Z_t)(\gamma_s + Z_s)]$, standard model contributions due to the t-channel and (s,t) interference. This term will be called 't-channel' for short,

$2\,\Re e\,[(\gamma_t + Z_t)C]$, interference between the standard model t-channel exchange amplitude and the contact term. In this expression the contribution of Z_t will be neglected since $|Z_t| << |\gamma_t|$.

The differential cross section for the reaction $e^+e^- \to \ell^+\ell^-$ including all terms except the 't-channel' is calculated in the improved Born approximation and has the form :

$$\frac{d\sigma}{d\Omega}^{Born} = a(s,\Lambda)(1+\cos^2\theta) + b(s,\Lambda)\cos\theta + c(s,\Lambda) + d(\cos\theta,\Lambda).$$

The coefficients $a(s,\Lambda)$, $b(s,\Lambda)$, $c(s,\Lambda)$ and $d(\cos\theta,\Lambda)$ are given by

$$\begin{aligned}
a(s,\Lambda) &= a_0(s) + \frac{1}{\Lambda^2}a_1(s) + \frac{1}{\Lambda^4}a_2(s) \\
b(s,\Lambda) &= b_0(s) + \frac{1}{\Lambda^2}b_1(s) + \frac{1}{\Lambda^4}b_2(s) \\
c(s,\Lambda) &= \delta\,\frac{1}{\Lambda^4}\,\frac{s}{4}\,(\eta_{LR}^2 + \eta_{RL}^2) \\
d(\cos\theta,\Lambda) &= -\delta\,\frac{\alpha}{\Lambda^2}\left((\eta_{LR}+\eta_{RL})\frac{1}{1-\cos\theta} + \frac{1}{2}(\eta_{LL}+\eta_{RR})\frac{(1+\cos\theta)^2}{1-\cos\theta}\right)
\end{aligned}$$

and

$$\delta = \begin{cases} 1 & \text{for electrons} \\ 0 & \text{for muons and taus.} \end{cases}$$

The differential cross section for all leptons combined is taken as the sum of those for individual lepton flavours, assuming a universal energy scale Λ.

The coefficients $a(s,\Lambda)$ and $b(s,\Lambda)$ have been decomposed into three terms due to standard model (subscript 0), contact interaction (2) and their interference (1) :

$$\left\{\begin{array}{lcl} a_0(s) & = & \frac{\alpha^2}{4s}\left[1+2\,v_\ell^2 \Re e\,\chi(s)+(v_\ell^2+a_\ell^2)^2|\chi(s)|^2\right] \\ a_1(s) & = & \frac{\alpha}{8}\left\{[\eta_{RL}+\eta_{LR}+(1+\delta)(\eta_{LL}+\eta_{RR})]+\right. \\ & & \qquad \Re e\,\chi(s)\,[(v_\ell^2-a_\ell^2)(\eta_{RL}+\eta_{LR})+ \\ & & \left.\qquad (1+\delta)(v_\ell-a_\ell)^2\eta_{RR}+(1+\delta)(v_\ell+a_\ell)^2\eta_{LL}]\right\} \\ a_2(s) & = & \frac{s}{16}\left[\eta_{RL}^2+\eta_{LR}^2+(1+\delta)^2(\eta_{RR}^2+\eta_{LL}^2)\right] \end{array}\right.$$

$$\left\{\begin{array}{lcl} b_0(s) & = & \frac{\alpha^2}{2s}\left[2a_\ell^2 \Re e\chi(s)+4v_\ell^2a_\ell^2|\chi(s)|^2\right] \\ b_1(s) & = & \frac{\alpha}{4}\left\{[-\eta_{RL}-\eta_{LR}+(1+\delta)(\eta_{LL}+\eta_{RR})]+\right. \\ & & \qquad \Re e\,\chi(s)\,[-(v_\ell^2-a_\ell^2)(\eta_{RL}+\eta_{LR})+ \\ & & \left.\qquad (1+\delta)(v_\ell-a_\ell)^2\eta_{RR}+(1+\delta)(v_\ell+a_\ell)^2\eta_{LL}]\right\} \\ b_2(s) & = & \frac{s}{8}\left[-\eta_{RL}^2-\eta_{LR}^2+(1+\delta)^2(\eta_{RR}^2+\eta_{LL}^2)\right]. \end{array}\right.$$

In these formulae, $\chi(s)$ is the Z propagator with s-dependent width : $\chi(s) = s(s-\mathrm{M_Z^2}+\mathrm{i}\,s\Gamma_\mathrm{Z}/\mathrm{M_Z})^{-1}$. The coupling α is taken equal to $\alpha(\mathrm{M_Z^2})$ except in the coefficient $d(\cos\theta,\Lambda)$ which is dominated by lower momentum transfer and where the value $\alpha(0)$ is used. The standard model axial and vector effective couplings a_ℓ and v_ℓ are:

$$\begin{array}{rcl} v_\ell & = & \left(\frac{G_F\mathrm{M_Z^2}}{2\sqrt{2}\pi\alpha(\mathrm{M_Z^2})}\right)^{1/2}\sqrt{\rho^{eff}(\mathrm{M_Z^2})}\left(I_3^\ell-2Q_\ell\sin^2\theta_\mathrm{W}^{eff}(\mathrm{M_Z^2})\right)\,, \\ a_\ell & = & \left(\frac{G_F\mathrm{M_Z^2}}{2\sqrt{2}\pi\alpha(\mathrm{M_Z^2})}\right)^{1/2}\sqrt{\rho^{eff}(\mathrm{M_Z^2})}I_3^\ell\,. \end{array}$$

The definitions of $\rho^{eff}(\mathrm{M_Z^2})$ and $\sin^2\theta_W^{eff}(\mathrm{M_Z^2})$ are the same as the ones used in [7] and [8].

Model predictions are corrected for initial state radiation effects according to [9]. Hard photon radiation is calculated up to order α^2 and the leading soft and virtual corrections are summed over all orders by the exponentiation technique. Each of the coefficients a, b and c is convoluted with the radiator function $H(x,s)$ where x is the fraction of energy lost by the radiation and s is the LEP energy squared. The resulting new coefficients are denoted by the corresponding capital letters, for example

$$A_0(s) = \int_0^{x_{\max}} H(x,s)a_0(s(1-x))dx.$$

The coefficient $d(\cos\theta)$ is energy independent and remains unchanged. The final expression for the differential cross section ('t-channel' excluded) is

$$\frac{d\sigma}{d\Omega} = A\,(s,\Lambda)(1+\cos^2\theta) + B\,(s,\Lambda)\cos\theta + C\,(s,\Lambda) + d\,(\cos\theta,\Lambda).$$

The standard model contributions to the Bhabha scattering due to the t-channel photon and Z exchange and to the interference between t and s channels are calculated using the program ALIBABA [10]. The intrinsic accuracy of the program due to missing contributions to the Bhabha scattering cross section is 0.5% as explained in [11].

2.2 Experimental data

This section contains a description of the experimental procedure which has led to the determination of the differential cross sections for the lepton pair production reactions. Four data samples are selected according to criteria described in [7, 11]:

$$\begin{aligned} e^+e^- &\to e^+e^- \\ e^+e^- &\to \mu^+\mu^- \\ e^+e^- &\to \tau^+\tau^- \\ e^+e^- &\to \ell^+\ell^-. \end{aligned}$$

The selection of the $\ell^+\ell^-$ events is done without distinguishing the lepton flavour in order to avoid systematic errors due to wrong flavour assignment. The total cumulated luminosity used in this analysis amounts to 19.7 pb^{-1} and is distributed over 12 different LEP operating energies, with 60% of it at the Z peak. Table 2 gives the values of the luminosity with the statistical errors, the numbers of collected events at each energy and the values of systematic errors. The systematic error on luminosity of 0.55% is due to theoretical and experimental uncertainties of the small-angle Bhabha cross section [12]. The error on the selection efficiency of each reaction is independent of energy and angle.[1]

The angular distributions are expressed as a function of the cosine of the scattering angle θ defined as :

$$\cos\theta = \frac{\cos\frac{1}{2}(\theta_1 + \pi - \theta_2)}{\cos\frac{1}{2}(\theta_1 - \pi + \theta_2)}$$

where θ_1 is the emission angle of the lepton and θ_2 of the antilepton, measured in the laboratory frame with respect to the incident electron. The angle θ has the advantage of being insensitive to initial state collinear photon radiation. Angular distributions are determined in 9 intervals of $\Delta\cos\theta = 0.2$ over the range $-0.9 < \cos\theta < 0.9$. In the experimental selection the acollinearity angle between the two leptons was required to

[1] Contrary to what was done in [7], here the t-channel was not subtracted for e^+e^- and $\ell^+\ell^-$ final states and therefore the systematic errors are smaller.

$\sqrt{s}$ (GeV)	Luminosity (nb^{-1})		e^+e^-	$\mu^+\mu^-$	$\tau^+\tau^-$	$\ell^+\ell^-$
88.25	590.7 $\pm$	4.6	534	98	92	757
88.50	668.9 $\pm$	4.9	649	142	142	950
89.25	566.8 $\pm$	4.5	609	216	179	1 035
89.50	799.8 $\pm$	5.4	979	356	277	1 667
90.25	1 275.3 $\pm$	4.4	1 979	910	859	3 900
91.25	11 636.7 $\pm$	20.3	21 001	13 816	12 660	49 270
92.00	697.6 $\pm$	5.2	930	696	539	2 363
92.25	668.0 $\pm$	5.1	783	463	514	1 934
93.00	680.5 $\pm$	5.2	541	369	335	1 308
93.25	640.2 $\pm$	5.1	509	313	284	1 153
93.75	771.3 $\pm$	5.6	512	321	285	1 149
94.25	708.6 $\pm$	5.3	404	228	205	891
Total	19 704.6 $\pm$	28.4	29 430	17 928	16 371	66 377
syst. error (%)	0.55		0.4	0.5	0.6	0.2

Table 2: Luminosities with statistical errors, number of events in the interval $|\cos\theta| < 0.9$ used in the analysis and systematic errors on the luminosity and on the event selection.

be smaller than 20°. The effect of this cut was evaluated with the KORALZ program [13] at each LEP energy.

For each reaction the background is subtracted and the corrections for the acollinearity cut and selection inefficiency are applied. The differential cross sections obtained after all corrections are plotted in figures 2–5 for the four reactions studied. The errors are only statistical.

2.3 Standard model predictions and comparison with the data

To determine the contribution of the contact terms in the reaction $e^+e^- \to \ell^+\ell^-$, one has first to evaluate the prediction of the standard model. The values of the four parameters M_Z, Γ_Z, $\sin^2\theta_W^{eff}(M_Z^2)$ and $\rho^{eff}(M_Z^2)$ should be as accurate as possible and obtained without making use of the lepton final states.

The values of the Z mass and width are taken as the averages of the measurements of the four LEP experiments: $M_Z = (91.175 \pm 0.021)$ GeV/c^2, $\Gamma_Z = (2.487 \pm 0.010)$ GeV/c^2 [8]. These measurements are dominated by hadronic final states. Contact interactions between quark and electrons would induce a shift of the Z mass depending on the value of the related energy scale [3]. Such possible shift is assumed to be negligible.

The parameters $\sin^2\theta_W^{eff}(M_Z^2)$ and $\rho^{eff}(M_Z^2)$ are deduced [14] through a determination of the top quark mass by a fit of the standard model parameters to the Z mass, W mass as measured in $p\bar{p}$ collisions [15], and the ratio M_W/M_Z measured in νN experiments [16].

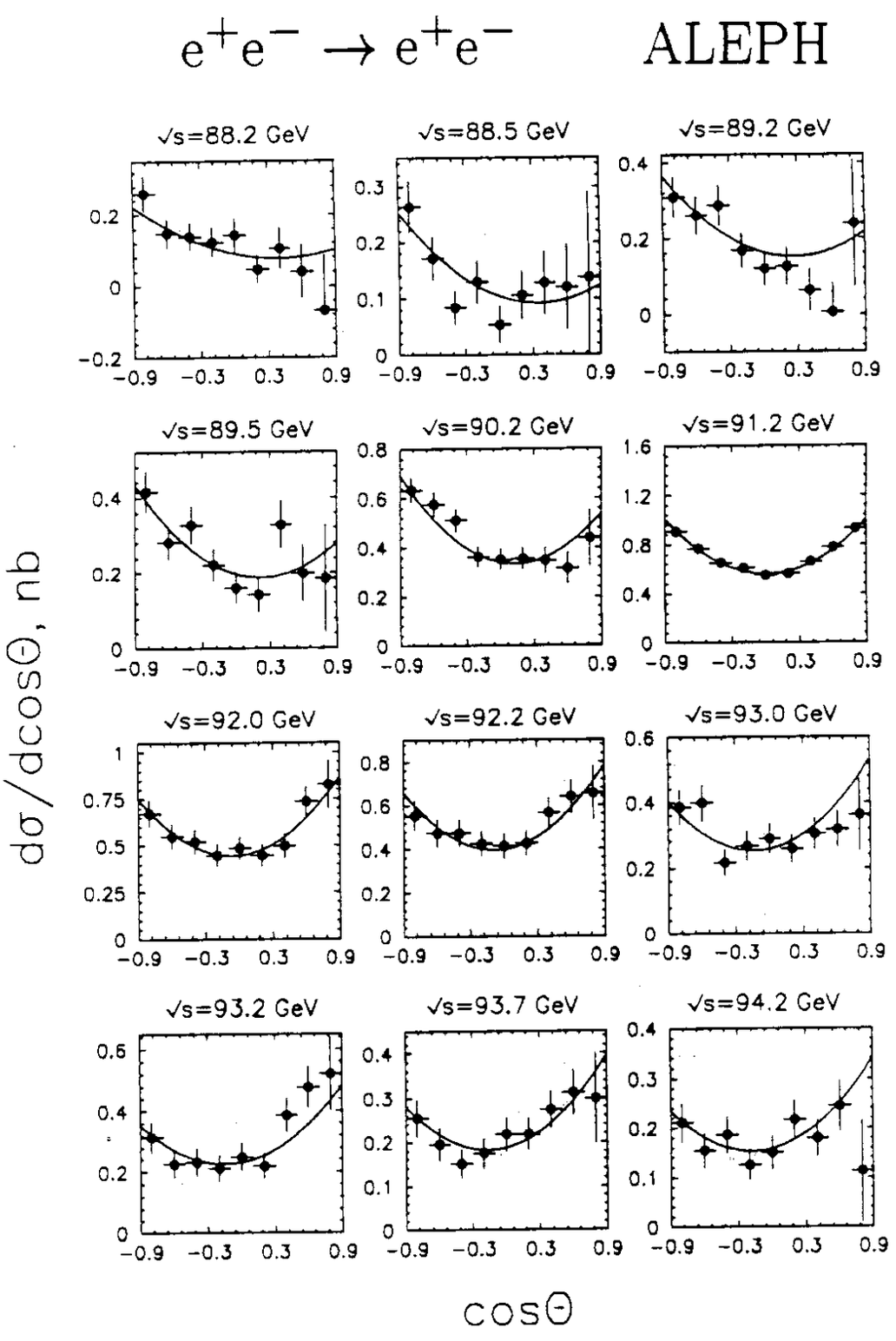

Figure 2: Differential cross sections for the reaction $e^+e^- \to e^+e^-$ at various LEP energies. The curves are the standard model predictions. The t-channel contribution is subtracted both from the data and from the standard model.

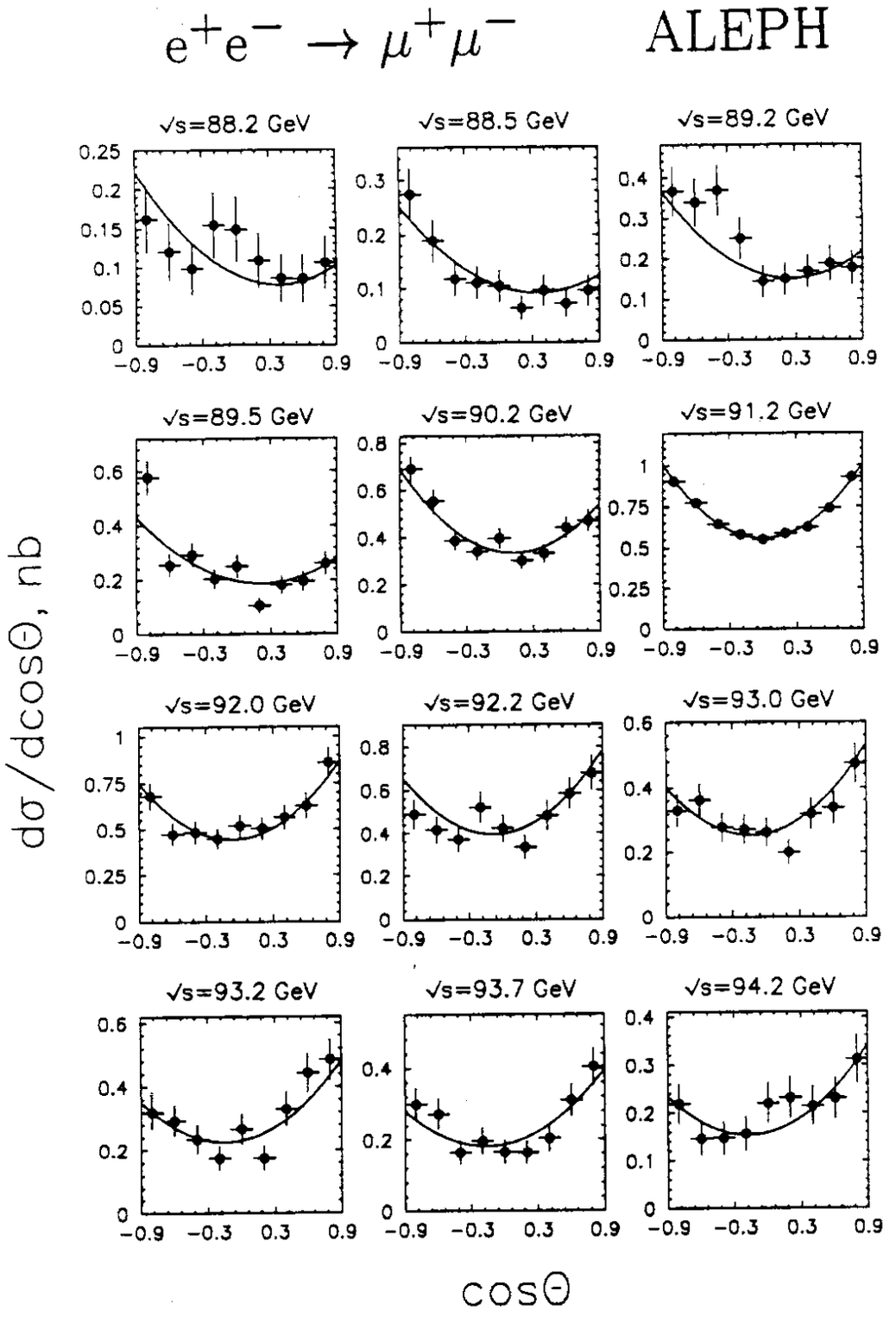

Figure 3: Differential cross sections for the reaction $e^+e^- \to \mu^+\mu^-$ at various LEP energies. The curves are the standard model predictions.

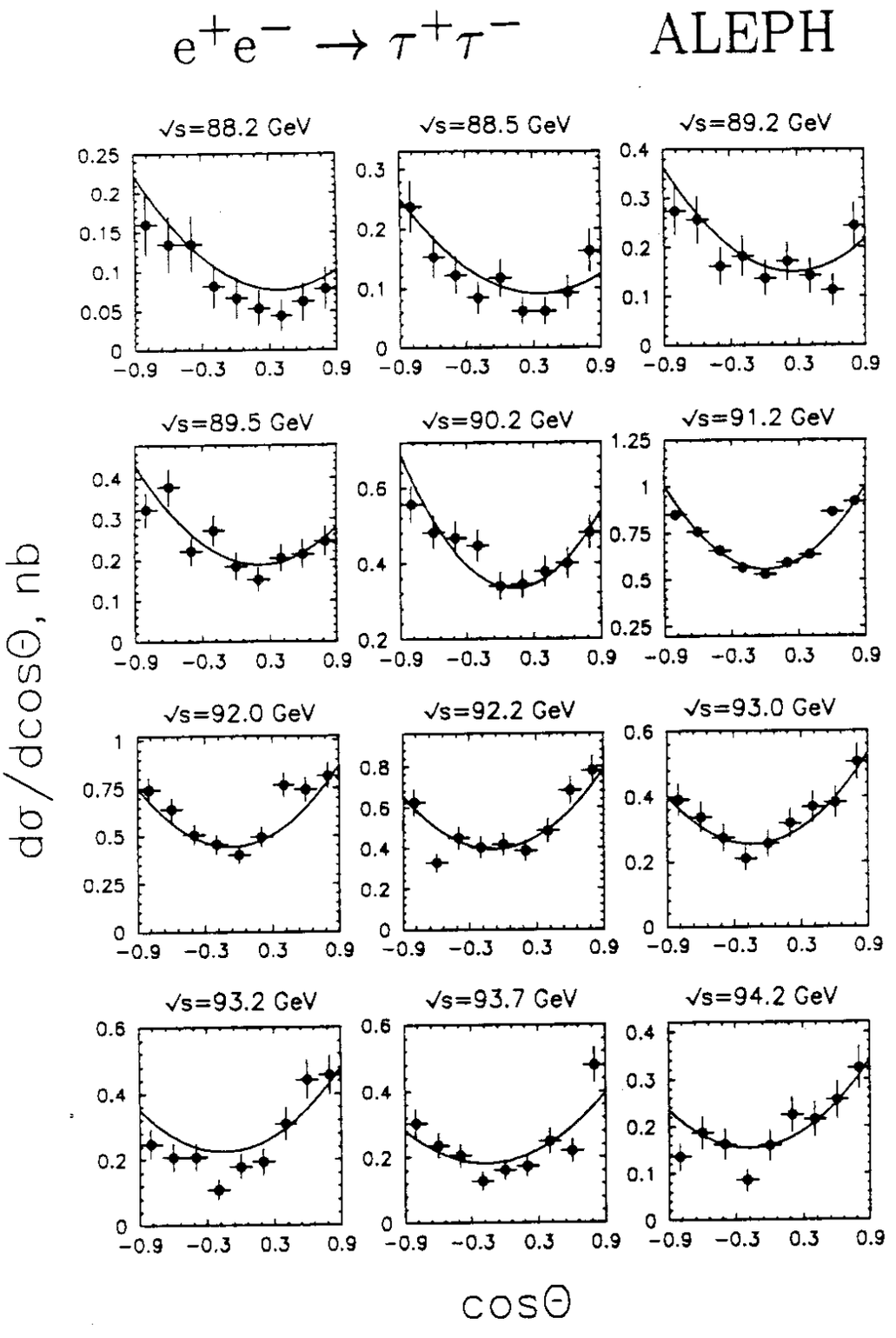

Figure 4: Differential cross sections for the reaction $e^+e^- \to \tau^+\tau^-$ at various LEP energies. The curves are the standard model predictions.

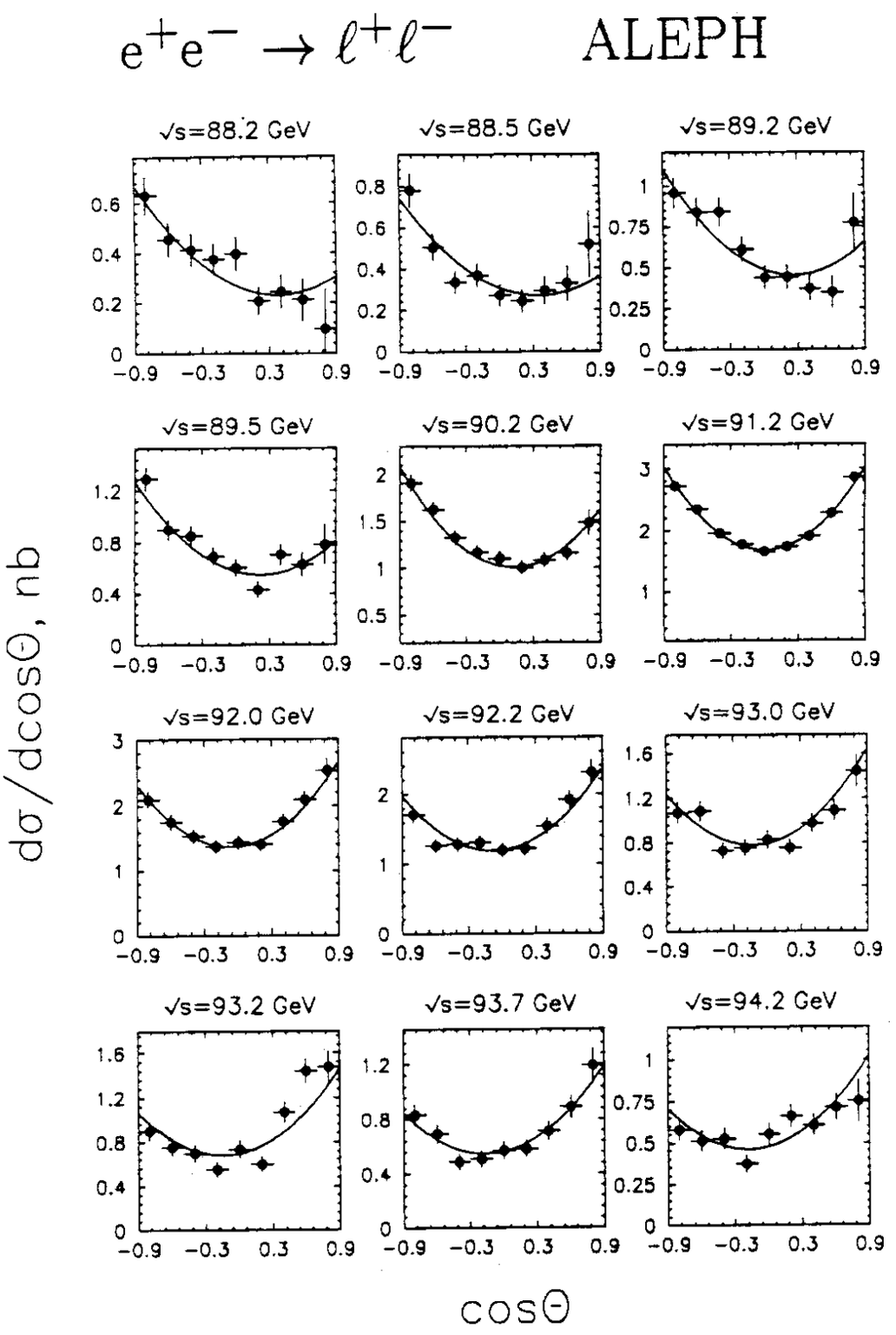

Figure 5: Differential cross sections for the reaction $e^+e^- \to \ell^+\ell^-$ at various LEP energies. The curves are the standard model predictions. The t-channel contribution is subtracted both from the data and from the standard model.

Measurements of $\sin^2\theta_W^{eff}(M_Z^2)$ with data from LEP are deliberately left out in order to obtain an estimate of the standard model parameters independent of the data to be fitted. Three values of the unknown Higgs mass are used: 50, 300 and 1000 GeV/c^2. The corresponding values of M_{top}, $\sin^2\theta_W^{eff}(M_Z^2)$ and $\rho^{eff}(M_Z^2)$ are listed in table 3.

M_{top} (GeV/c^2)	190	146	93
M_{Higgs} (GeV/c^2)	1000	300	50
$\sin^2\theta_W^{eff}(M_Z^2)$	0.2321	0.2330	0.2334
$\rho^{eff}(M_Z^2)$	1.0056	1.0026	0.9997

Table 3: Values of the standard model parameters determined from electroweak data.

The central set of values with $M_{top} = 146$ GeV/c^2 is used to calculate the predictions of the standard model according to the formulae of section 2.1. These values are kept fixed in the fits of the models to the differential cross section data. The other two sets are used later to test the sensitivity of the fit results to the standard model parameters.

The predictions of the standard model alone calculated with all the parameters fixed at the values given above are in good agreement with the measured differential cross sections as shown in figures 2–5. For 108 degrees of freedom, the values of χ^2 are 82, 111, 141 and 120 for the channels e^+e^-, $\mu^+\mu^-$, $\tau^+\tau^-$ and $\ell^+\ell^-$, respectively.

2.4 Fits of the contact terms to the data

A possible contribution of the contact terms to the experimental differential cross sections is determined by a binned maximum likelihood fit. The input data are expressed in terms of the number of events detected in each bin of $\cos\theta$ at each energy. The corresponding expected number of events is calculated taking into account the theoretical model, the measured luminosities, the detector efficiency and analysis cuts. The fit includes all sources of normalisation errors due to systematic effects.

The contact term amplitude is proportional to the parameter

$$\epsilon = 1/\Lambda^2$$

which was left free in the fit. The parameter ϵ is expected to have a Gaussian error and for this reason it is prefered over Λ. The only other parameters determined in the fit are the normalizations n_0, n_k, n_t which were allowed to deviate from unity within their errors:

Δn_0, the overall systematic error due to the luminosity and the selection efficiency errors as given in table 2, added in quadrature,

Δn_k, the relative statistical error of the luminosity L_k at each energy $\sqrt{s_k}$,

Δn_t, the uncertainty in the t-channel calculation (0.6% at the Z peak or below it and 1.2% above), due to the limited accuracy of the program and to the uncertainties of the Z mass and width which induce errors on the (s,t) interference term.

The likelihood function is defined as:

$$\mathcal{L} = f\, g(n_0) \prod_{k=1}^{12} g(n_k) \prod_{i=1}^{9} \mathcal{P}\left(N_{ik}^{\mathrm{DATA}}, N_{ik}^{\mathrm{PRED}}(\Lambda)\right) ,$$

where the index k runs over LEP energies and i numbers the cos θ bins. $g(n)$ is the Gaussian probability distribution of the variable n with mean value 1 and standard deviation Δn. $f = g(n_t)$ for electrons and 'all leptons' and $f = 1$ otherwise.

$\mathcal{P}$ is the Poisson probability of observing N_{ik}^{DATA} events while $N_{ik}^{\mathrm{PRED}}(\Lambda)$ are expected. N_{ik}^{DATA} is the number of events after background subtraction but without any other correction. The expected number of events $N_{ik}^{\mathrm{PRED}}(\Lambda)$ is given by

$$N_{ik}^{\mathrm{PRED}}(\Lambda) = n_0 n_k L_k \left[\sigma_{ik}(\Lambda) a_{ik} + \delta\, n_t \sigma_{ik}^t\right] e_{ik} ,$$

where:

σ_{ik} is the previously derived differential cross section without the t-channel contribution at a given energy $\sqrt{s_k}$, integrated over the cosθ bin i and the azimuthal angle,

σ_{ik}^t is the t-channel contribution inside the acollinearity cut,

δ=1 for electrons and 'all leptons' and 0 otherwise,

e_{ik} is the experimental efficiency and a_{ik} is the correction for the acollinearity cut.

The maximum likelihood method does not allow the quality of the fit to be estimated easily. Therefore the value of χ^2 is calculated after each fit, after inserting the fitted values of the parameters into the expression of $N_{ik}^{\mathrm{PRED}}(\Lambda)$.

2.5 Results of contact term fits

The contact term models are now fitted to the data in order to set limits on the energy scale Λ. The parameter ε is adjusted by the fit together with the normalization parameters defined before. The fitted values of ε and its one standard deviation errors σ^+ and σ^- are listed in table 4 for the models LL, RR, VV, AA and LR; the RL model is indistinguishable from LR since the predictions are symmetric with respect to the exchange of η_{RL} and η_{LR}. No significant deviation of ε from zero is found for any of the models and any lepton flavour. The normalization parameters are compatible with 1 and the values of χ^2 differ very little from the corresponding values for the standard model comparison.

Electrons	$\varepsilon^{+\sigma^+}_{-\sigma^-}$ (TeV^{-2})	λ (TeV)	Λ^+ (TeV)	Λ^- (TeV)
LL	$0.115^{+0.147}_{-0.145}$	2.0	1.6	2.0
RR	$0.120^{+0.170}_{-0.166}$	1.9	1.5	1.9
VV	$0.046^{+0.050}_{-0.050}$	3.5	2.8	3.5
AA	$0.005^{+0.071}_{-0.072}$	2.9	2.8	2.9
LR	$0.134^{+0.177}_{-0.174}$	1.8	1.5	1.8

Muons	$\varepsilon^{+\sigma^+}_{-\sigma^-}$ (TeV^{-2})	λ (TeV)	Λ^+ (TeV)	Λ^- (TeV)
LL	$0.144^{+0.249}_{-0.248}$	1.5	1.3	1.5
RR	$0.171^{+0.327}_{-0.325}$	1.3	1.1	1.3
VV	$0.202^{+0.111}_{-0.111}$	2.3	1.6	2.3
AA	$-0.065^{+0.087}_{-0.087}$	2.6	2.6	2.1
LR	$0.431^{+0.257}_{-0.260}$	1.5	1.0	1.5

Taus	$\varepsilon^{+\sigma^+}_{-\sigma^-}$ (TeV^{-2})	λ (TeV)	Λ^+ (TeV)	Λ^- (TeV)
LL	$0.392^{+0.271}_{-0.269}$	1.5	1.0	1.5
RR	$0.603^{+0.372}_{-0.372}$	1.2	0.9	1.2
VV	$-0.064^{+0.112}_{-0.112}$	2.3	2.3	2.0
AA	$0.198^{+0.089}_{-0.089}$	2.6	1.7	2.6
LR	$-0.463^{+0.251}_{-0.253}$	1.5	1.5	1.0

Leptons	$\varepsilon^{+\sigma^+}_{-\sigma^-}$ (TeV^{-2})	λ (TeV)	Λ^+ (TeV)	Λ^- (TeV)
LL	$-0.071^{+0.068}_{-0.068}$	3.0	3.0	2.3
RR	$-0.087^{+0.072}_{-0.072}$	2.9	2.9	2.2
VV	$-0.010^{+0.028}_{-0.028}$	4.7	4.7	4.2
AA	$-0.070^{+0.037}_{-0.038}$	4.0	4.0	2.7
LR	$0.171^{+0.135}_{-0.136}$	2.1	1.6	2.1

Table 4: Results of the contact term fits to the ALEPH data for reactions $e^+e^- \to \ell^+\ell^-$. The contribution of the contact term, ε, is given with one standard deviation errors. λ is the resolving power and Λ^+ and Λ^- are the 95% c.l. limits on the energy scale Λ corresponding to each sign of the contact amplitude.

In order to test the sensitivity of the results to variation of the standard model parameters, the contact term fits are repeated changing the values of the Z mass and width within experimental errors and using the two extreme sets of values of $\sin^2\theta_W^{eff}(M_Z^2)$ and $\rho^{eff}(M_Z^2)$ given in table 3. The values of ε so determined differ from the central value of ε by much less than one standard deviation for all reactions and all models. Therefore the errors on ε due to the uncertainty of the standard model parameters are ignored.

Results of the fits for three selected energies: 89.5, 91.2 and 93.7 GeV are plotted in figures 6-7 for electrons and muons and for all models except RR which is very similar to LL. The contact term model predictions and the experimental data are divided by the predictions of the standard model alone. In the plot for electrons the t-channel contribution is subtracted from the data and omitted from the model predictions. The pair of curves in each plot shows the maximum allowed positive and negative contributions of the contact term at 95% c.l. calculated by setting ε to the values $\varepsilon + 1.64\sigma^+$ and $\varepsilon - 1.64\sigma^-$, respectively.

Limits on the compositeness scale Λ are deduced at 95 % c.l. from the formulae

$$\Lambda^+ = \left(\varepsilon + 1.64\ \sigma^+\right)^{-1/2} \qquad \Lambda^- = \left(-\varepsilon + 1.64\ \sigma^-\right)^{-1/2}$$

where Λ^+ and Λ^- correspond to the positive or negative sign of the contact term amplitude.

It has been pointed out [17, 18] that when Λ is undefined (negative value under the square root) or larger than a certain value which is a measure of the experimental sensitivity, then the limit should be set equal to this value. Following this idea, the limits $\Lambda^\pm$ are bounded by the resolving power λ defined as the one-sided 95% c.l. error on ε in the absence of contact terms ($\varepsilon = 0$) :

$$\lambda = (1.64\ \sigma)^{-1/2}$$

where σ is the parabolic one-standard-deviation error on ε. The resolving power is a measure of the sensitivity of an experiment to a given model; it depends on the statistics N like $N^{1/4}$ and on the nature of the model.

Limits on Λ deduced from the fits and restricted to the region $\Lambda^\pm \leq \lambda$ are listed in table 4 for the contact terms $eeee$, $ee\mu\mu$, $ee\tau\tau$ and the flavour-independent four-lepton contact interaction. Values of Λ smaller than these limits are excluded at 95% c.l. The limits vary between 0.9 and 4.7 TeV depending on the model and on lepton flavour.

Information on the contact term is provided in this analysis both by the angular distribution and by the absolute cross section. The sensitivities of the fits to these quantities have been studied by varying the normalization errors. For most flavours and models the two sensitivities are comparable. For the AA model, especially for muons and taus, the fit is dominated by the normalization because of the flatness of the relative contribution of the contact term to the standard model angular distribution.

The results obtained for the e^+e^- and $\ell^+\ell^-$ final states are more stringent than those for $\mu^+\mu^-$ and $\tau^+\tau^-$. This is a consequence of the real nature of the t-channel

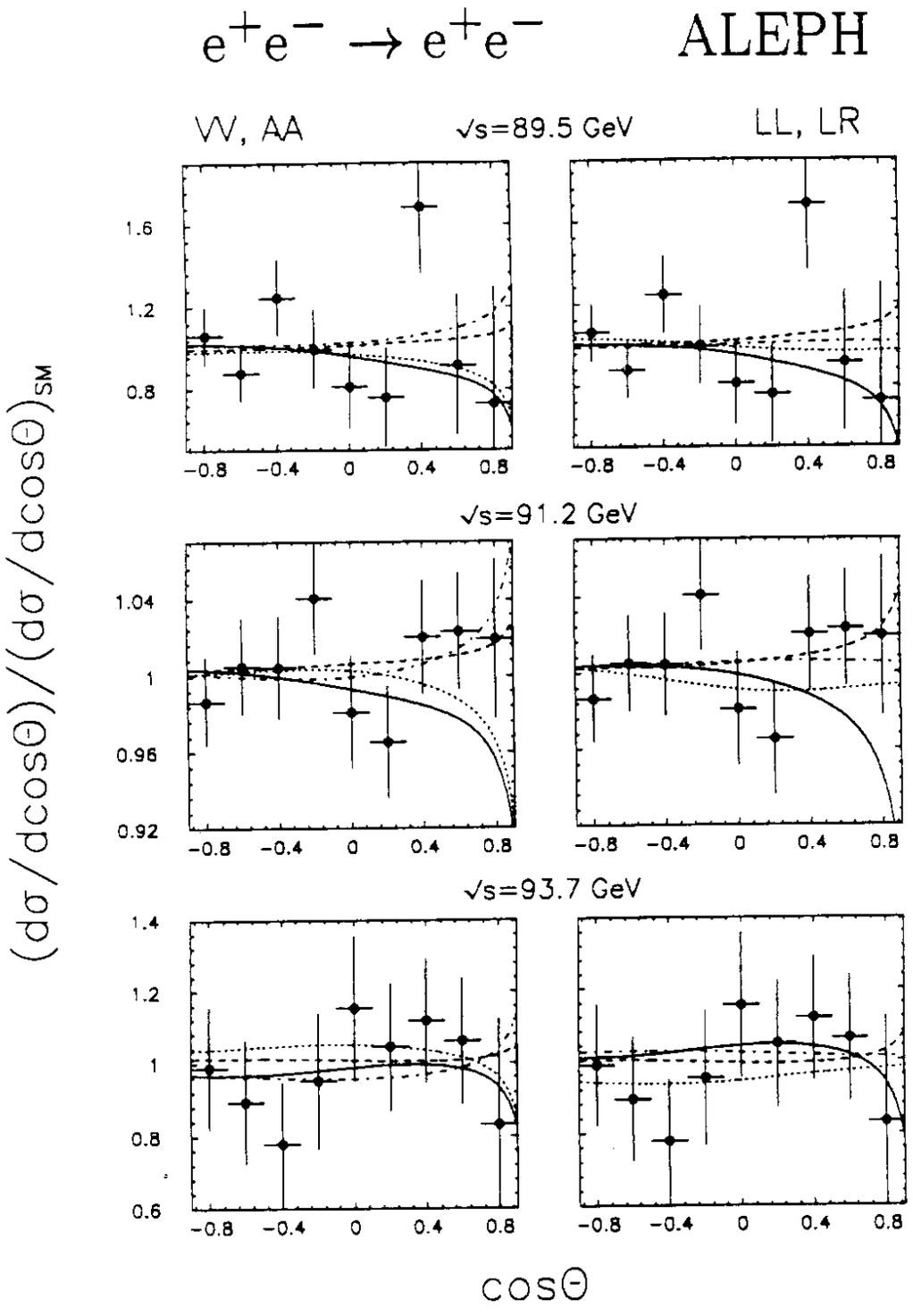

Figure 6: Results of the fits of contact models for the reaction $e^+e^- \to e^+e^-$. The data points are the measured differential cross sections divided by the standard model predictions. The t-channel contribution is subtracted. The curves are the maximum allowed deviations at 95% c.l. Left-hand side: continuous lines Λ^+_{VV}, dashed Λ^-_{VV}, dotted Λ^+_{AA}, dash-dotted: Λ^-_{AA}. The corresponding lines on the right-hand side are for Λ^+_{LL}, Λ^-_{LL}, Λ^+_{LR} and Λ^-_{LR}.

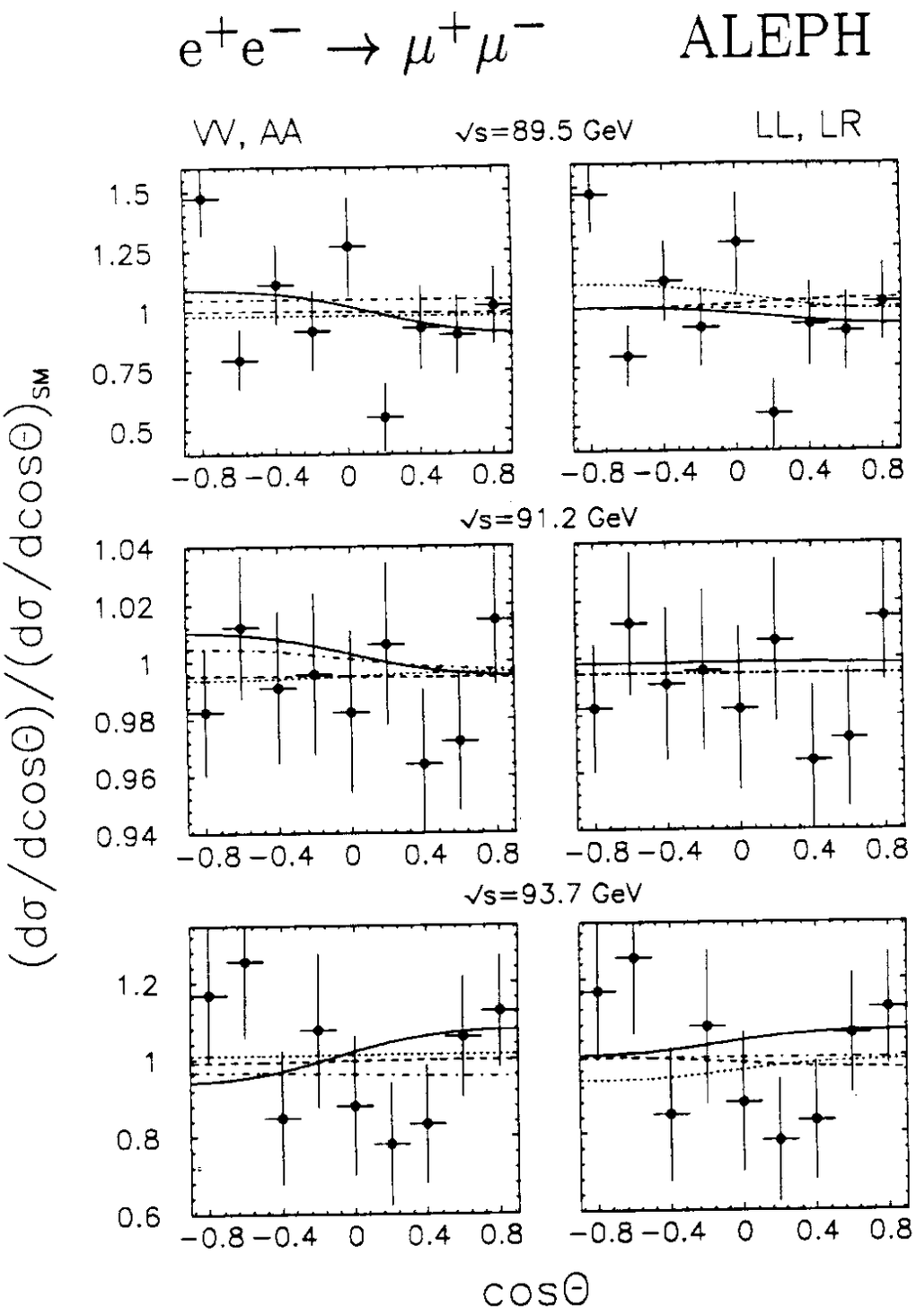

Figure 7: Results of the fits of contact models for the reaction $e^+e^- \to \mu^+\mu^-$. The data points are the measured differential cross sections divided by the standard model predictions. The curves are the maximum allowed deviations at 95% c.l. Left-hand side: continuous lines Λ^+_{VV}, dashed Λ^-_{VV}, dotted Λ^+_{AA}, dash-dotted: Λ^-_{AA}. The corresponding lines on the right-hand side are for Λ^+_{LL}, Λ^-_{LL}, Λ^+_{LR} and Λ^-_{LR}.

photon exchange amplitude which interferes with the real contact term amplitude. It can be seen in figure 6 that the expected contribution of the contact term models is indeed concentrated in the forward region. It is interesting to investigate the effect of the contact terms on small angle Bhabha scattering in the range covered by the luminometer. If appreciable, this contribution would affect the luminosity measurement (and all ALEPH cross sections) and should be included in the contact term fits for internal consistency. The magnitude of the effect is estimated by integrating the term $d(\cos\theta, \Lambda)$ over the acceptance of the luminometer, $57 < \theta < 110$ mrad, taking for each model the value of Λ equal to its 95% c.l. limit. The largest result is obtained for the model VV; it amounts to 12 pb and represents a negligible fraction (0.05%) of the Bhabha cross section in the same angular region [12].

2.6 Comparison with lower energies and discussion

Four-lepton contact terms have been studied in e^+e^- collisions at PEP, PETRA and TRISTAN. Results obtained at these machines from individual experiments are reinvestigated and combined together in ref. [18]. A comparison of the values of ϵ from various lower energy experiments [18, 19] and from this analysis is shown in figures 8–11 for each model and each lepton flavour. The results are then translated into the 95% c.l. limits on Λ and the constraint $\Lambda^{\pm} \leq \lambda$ is imposed in all cases. The values obtained are listed in table 5.

For electrons the ALEPH limits are higher than those from any other individual experiment for all models except LR, and they exceed the combined PEP/PETRA limit for the LL and RR models.

For the s-channel final states $\mu^+\mu^-$ and $\tau^+\tau^-$ ALEPH limits are comparable to or weaker than those at lower energies due to the dominance of the imaginary Z-exchange amplitude at LEP. Since Λ is large, contact terms are searched for via the interference with the standard model amplitude. Unlike at PEP/PETRA and TRISTAN energies, the interference almost vanishes at the Z peak where most of the data was taken. However this disadvantage is partly outweighed by high statistics and a precise luminosity measurement in this analysis.

The sensitivity to contact terms depends on the chiral structure of the standard model as well as of the contact term itself. At LEP the relative contribution of the AA model is flat in $\cos\theta$ for the s-channel reactions $\mu^+\mu^-$ and $\tau^+\tau^-$ while at PETRA the same is true for the VV model. Thus to some extent, the analyses performed at different energies are complementary.

The best presently available limits on four-lepton contact interactions from the combined results of ALEPH and lower energy experiments vary from 1.6 to 6.0 TeV at 95% c.l.

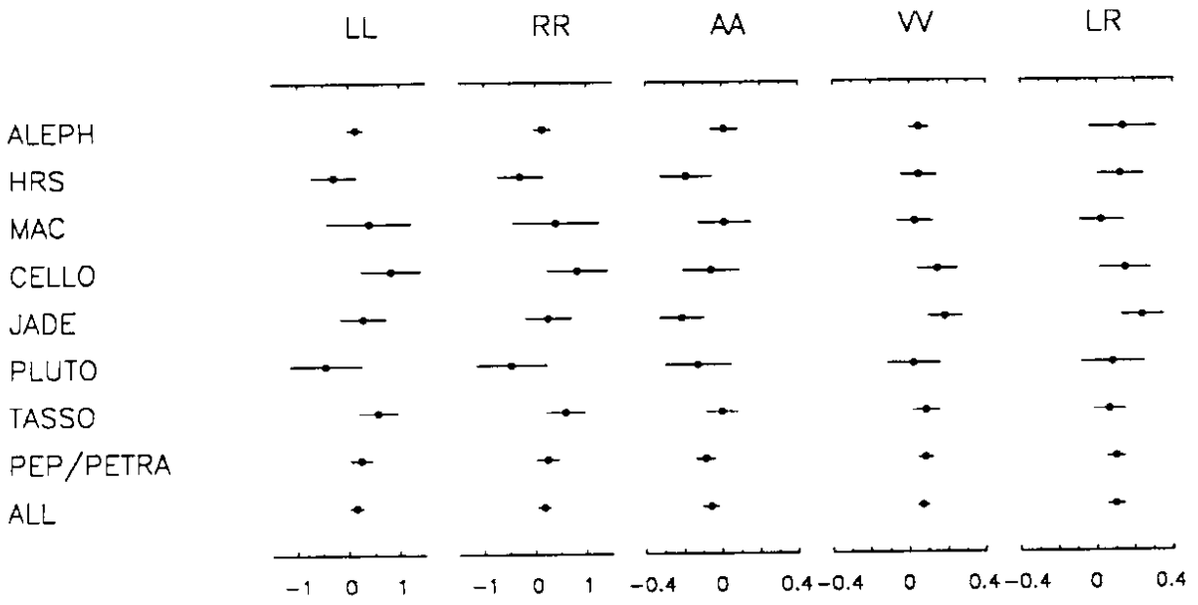

Figure 8: Values of ε (in TeV^{-2}) from the reaction $e^+e^- \to e^+e^-$ plotted with one standard deviation errors. 'ALL' is the weighted average of ALEPH and PEP/PETRA.

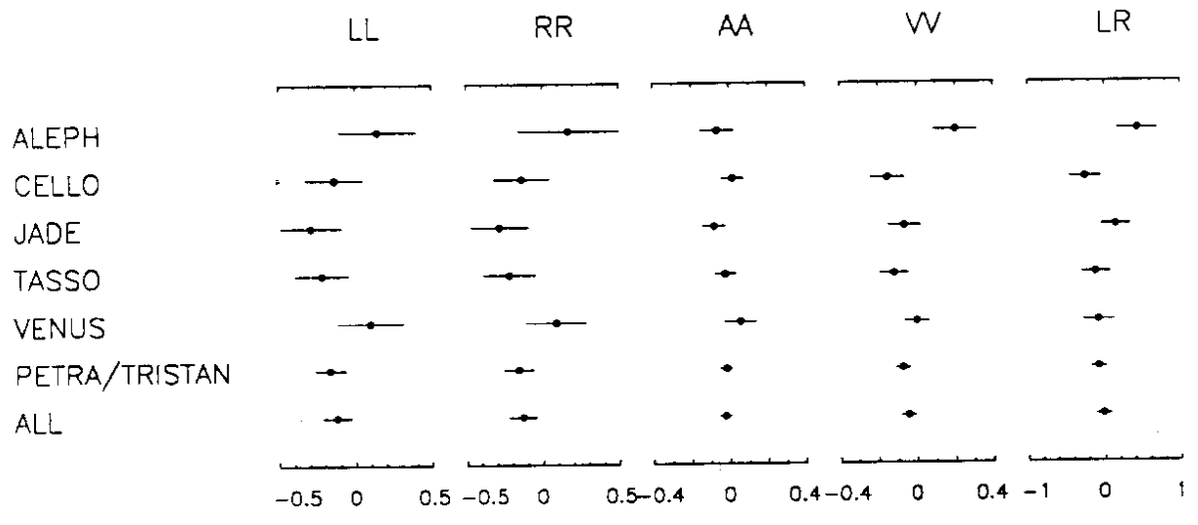

Figure 9: Values of ε (in TeV^{-2}) from the reaction $e^+e^- \to \mu^+\mu^-$ plotted with one standard deviation errors. 'ALL' is the weighted average of ALEPH and PETRA/TRISTAN.

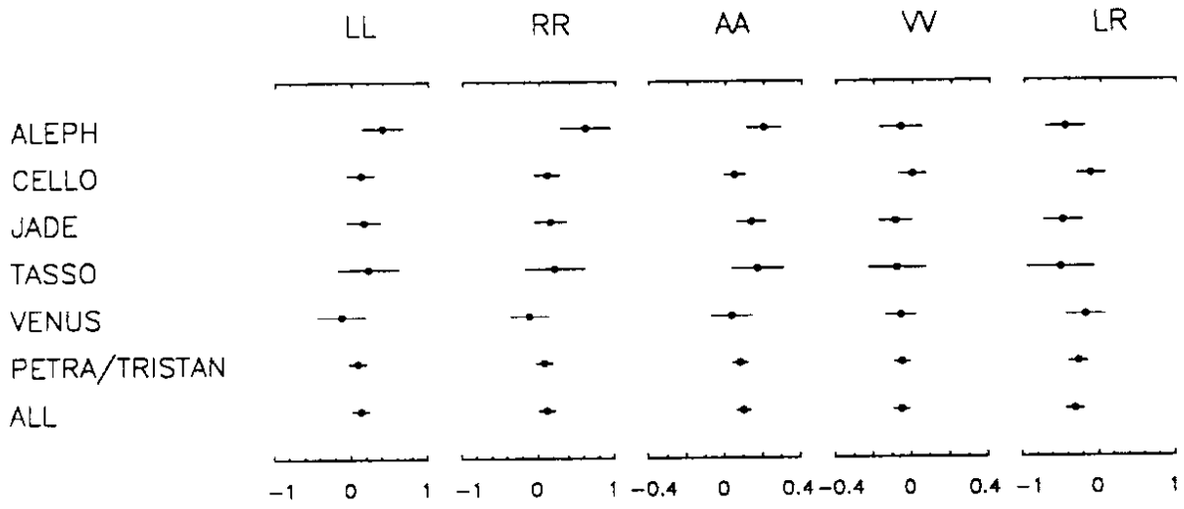

Figure 10: Values of ε (in TeV^{-2}) from the reaction $e^+e^- \to \tau^+\tau^-$ plotted with one standard deviation errors. 'ALL' is the weighted average of ALEPH and PETRA/TRISTAN.

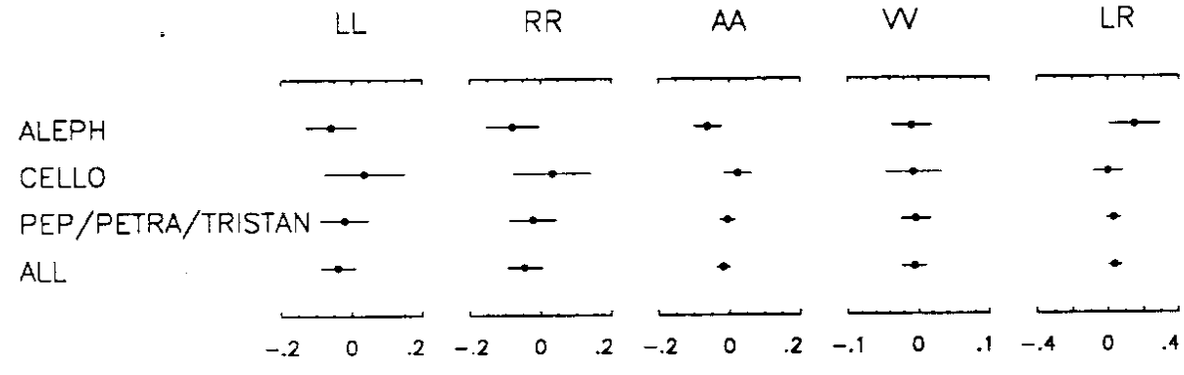

Figure 11: Values of ε (in TeV^{-2}) from the reaction $e^+e^- \to \ell^+\ell^-$ plotted with one standard deviation errors. 'ALL' is the weighted average of ALEPH and PEP/PETRA/TRISTAN.

	LL		RR		VV		AA		LR	
$eeee$	Λ^+	Λ^-	Λ^+	Λ^-	Λ^+	Λ^-	Λ^+	Λ^-	Λ^+	Λ^-
HRS	1.2	1.0	1.2	1.0	2.3	2.6	2.2	1.5	1.8	2.3
MAC	0.7	0.9	0.7	0.9	2.4	2.5	2.1	2.1	2.2	2.3
CELLO	0.7	1.0	0.7	1.0	1.8	2.5	2.1	1.8	1.7	2.2
JADE	1.0	1.2	1.0	1.2	1.8	2.6	2.4	1.6	1.6	2.4
PLUTO	0.9	1.0	1.2	0.8	2.1	2.2	2.0	1.6	1.8	2.0
TASSO	0.9	1.3	0.9	1.3	2.2	3.0	2.7	2.6	2.2	2.7
PEP/PETRA	1.3	1.7	1.3	1.7	2.6	4.1	3.5	2.4	2.4	3.6
ALEPH	1.6	2.0	1.5	1.9	2.8	3.5	2.8	2.9	1.5	1.8
ALL	1.6	2.2	1.6	2.1	2.8	4.5	3.9	2.8	2.3	3.7
$ee\mu\mu$										
CELLO	1.8	1.5	1.8	1.5	2.7	1.8	3.0	3.2	1.7	1.3
JADE	1.8	1.3	1.8	1.3	2.7	2.2	3.3	2.4	1.5	1.8
TASSO	1.9	1.4	1.9	1.4	2.9	2.0	3.3	3.0	1.9	1.5
VENUS	1.5	1.8	1.6	1.7	3.1	3.0	2.3	2.7	2.1	1.7
PETRA/TRISTAN	2.5	1.7	2.5	1.8	4.0	2.7	4.5	3.8	2.5	2.0
ALEPH	1.3	1.5	1.1	1.3	1.6	2.3	2.6	2.1	1.0	1.5
ALL	2.6	1.9	2.6	1.9	4.1	3.1	4.6	3.8	2.6	2.5
$ee\tau\tau$										
CELLO	1.6	1.8	1.6	1.9	2.9	2.9	2.6	3.2	1.8	1.5
JADE	1.4	1.6	1.4	1.6	2.7	2.1	2.0	2.8	1.6	1.1
TASSO	1.1	1.2	1.1	1.2	2.0	1.8	1.6	2.1	1.2	0.9
VENUS	1.5	1.1	1.5	1.2	2.8	2.3	2.2	2.4	1.6	1.3
PETRA/TRISTAN	1.9	2.2	1.9	2.3	3.8	2.9	2.6	3.9	2.2	1.5
ALEPH	1.0	1.5	0.9	1.2	2.3	2.0	1.7	2.6	1.5	1.0
ALL	1.8	2.3	1.8	2.3	3.9	2.9	2.5	4.0	2.3	1.4
four-lepton										
CELLO	2.1	2.3	2.1	2.3	3.7	3.2	3.3	3.9	2.6	2.4
PEP/PETRA/TRISTAN	3.0	2.7	3.1	2.8	5.4	5.1	5.3	5.0	3.3	4.1
ALEPH	3.0	2.3	2.9	2.2	4.7	4.2	4.0	2.7	1.6	2.1
ALL	3.5	2.8	3.5	2.7	6.0	5.4	5.7	4.4	3.1	4.1

Table 5: Limits on $\Lambda^{\pm}$ in TeV at 95% c.l. obtained in various experiments and the combined results. The constraint $\Lambda^{\pm} \leq \lambda$ is imposed in all cases.

3 Two-photon, two-electron contact terms

Contact interactions of two fermions and two-bosons are discussed in [4, 5]. For the $ee\gamma\gamma$ case the interaction Lagrangian can be written in the form

$$\mathcal{L}_{ee\gamma\gamma} = \frac{2ie^2}{\Lambda^4} F^{\mu\sigma} F^{\nu}_{\sigma} \left(\eta_L \overline{\psi^e_L} \gamma_\mu \partial_\nu \psi^e_L + \eta_R \overline{\psi^e_R} \gamma_\mu \partial_\nu \psi^e_R \right)$$

where the dimensions of the fields involved imply the 4th power of Λ. Table 6 defines 4×2 contact term models depending on the chirality of the electron current. As previously, the contact amplitude is real and both signs are possible.

Model	η_R	η_L
L	0	± 1
R	± 1	0
$L+R$	± 1	± 1
$L-R$	± 1	∓ 1

Table 6: Definition of the $ee\gamma\gamma$ contact models.

3.1 Differential cross section

The reaction $e^+e^- \to \gamma\gamma$ is purely electromagnetic and has been proposed as a suitable process to search for deviations from QED due to new phenomena at LEP [5]. In the contact term approach the photon pair production is described at the tree level by two QED graphs and the contact term diagram shown in fig. 12. The differential cross

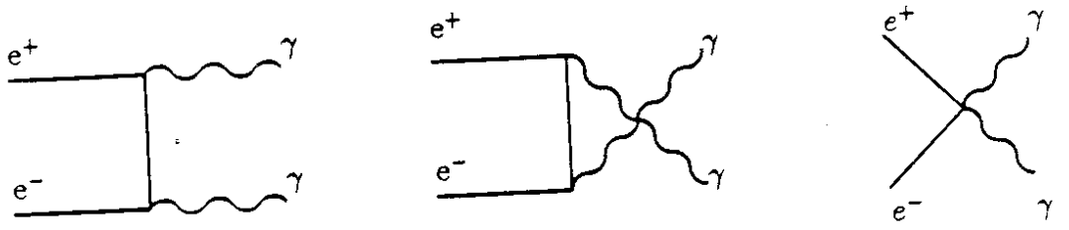

Figure 12: Diagrams contributing to the reaction $e^+e^- \to \gamma\gamma$

section in the Born approximation can be written as a sum:

$$\frac{d\sigma}{d\Omega} = \frac{\alpha^2}{s} \frac{1+\cos^2\theta}{1-\cos^2\theta} + \left(\frac{d\sigma}{d\Omega}\right)^{\text{CONTACT}}$$

The first term comes from QED and the second includes the contact term itself and its interference with QED. Depending on the chirality of the electron current and on the

sign of the (real) contact amplitude, the second term is given by one of the expressions:

$$\left(\frac{d\sigma}{d\Omega}\right)^{\mathrm{L,R}} = \pm\frac{\alpha^2 s}{4\Lambda^4}\,(1+\cos^2\theta) + \frac{\alpha^2 s^3}{32\Lambda^8}\,(1-\cos^4\theta)$$

$$\left(\frac{d\sigma}{d\Omega}\right)^{\mathrm{L+R}} = \pm\frac{\alpha^2 s}{2\Lambda^4}\,(1+\cos^2\theta) + \frac{\alpha^2 s^3}{16\Lambda^8}\,(1-\cos^4\theta)$$

$$\left(\frac{d\sigma}{d\Omega}\right)^{\mathrm{L-R}} = \frac{\alpha^2 s^3}{16\Lambda^8}\,(1-\cos^4\theta)$$

$$\left(\frac{d\sigma}{d\Omega}\right)^{cut-off} = \pm\frac{\alpha^2 s}{2\Lambda^4}\,(1+\cos^2\theta).$$

For every model two different Λ-scales are defined except for the $L-R$ model where the interference term vanishes. The dominant contribution comes from the interference term proportional to Λ^{-4}. Hence the model $L-R$ is less sensitive than other models with the same Λ. The last formula concerns the "cut-off" model [20] in which the deviation from QED is approximated by a form factor. The model predicts a cross section very similar to that of the $L+R$ model. The predictions of the R and L models are identical.

3.2 Experimental data and comparison with QED

Events are selected from a data sample of integrated luminosity 20.5 pb^{-1} by requiring at least two photons and no charged particles as described in [21]. In addition events with at least one photon and one e^+e^- pair for which the opening angle is smaller than 10° are included. Unresolved e^+e^- pairs giving rise to a single, doubly ionising track are accepted. Events with a e^+e^- pair are expected to come either from the reaction $e^+e^- \to \gamma\gamma(\gamma)$ in which one of the photons converts in the detector, or from Bhabha scattering with a very hard radiative photon.

The statistics for the reaction $e^+e^- \to \gamma\gamma$ is considerably smaller than for the lepton pair data and the QED and contact cross sections depend weakly on energy, therefore the data taken at 12 energies $\sqrt{s_k}$ is combined. The angular distribution is expressed in terms of the angle θ defined as for the charged leptons, θ_1 and θ_2 being the polar angles of the two most energetic photons. The acollinearity angle must be smaller than 60°. The angular region covered by this analysis extends up to $\cos\theta$=0.95.

QED predictions for the reaction $e^+e^- \to \gamma\gamma(\gamma)$ are calculated using the event generator of Berends and Kleiss [22] and full detector simulation. Radiative Bhabhas are simulated using the BABAMC event generator [23] and are expected to contribute 2% of the accepted cross section. The simulations are performed at the effective evergy $\sqrt{s_{eff}}$= 91.225 GeV defined as

$$s_{eff} = (\sum_k L_k)\,(\sum_k L_k/s_k)^{-1},$$

since the cross section behaves like s^{-1}.

The total number of detected events within the angular acceptance is 818 while 803.7 are expected. The normalization error, due to systematic and statistical uncertainties of the luminosity measurement and to the error on the selection efficiency, is estimated to be 1.2%. The results of the Monte Carlo simulations are used to determine the acceptance correction and to unfold the radiative correction effect, thus allowing the cross section at the Born level to be extracted from the observed events and luminosity. The correction a_i due to initial state radiation and to the acollinearity cut is determined at the generator level. The values of a_i are 1.1–1.2 depending on $\cos\theta$. The detection efficiency e_i is obtained from the full simulation including detector effects and analysis cuts. The value of the efficiency averaged over the geometrical acceptance equals 0.86.

The differential cross section averaged over all LEP energies is evaluated in 19 bins of $\cos\theta$ and compared in fig. 13 with QED prediction calculated at the Born level at the effective energy. The value of χ^2 is 16.3 for 19 degrees of freedom.

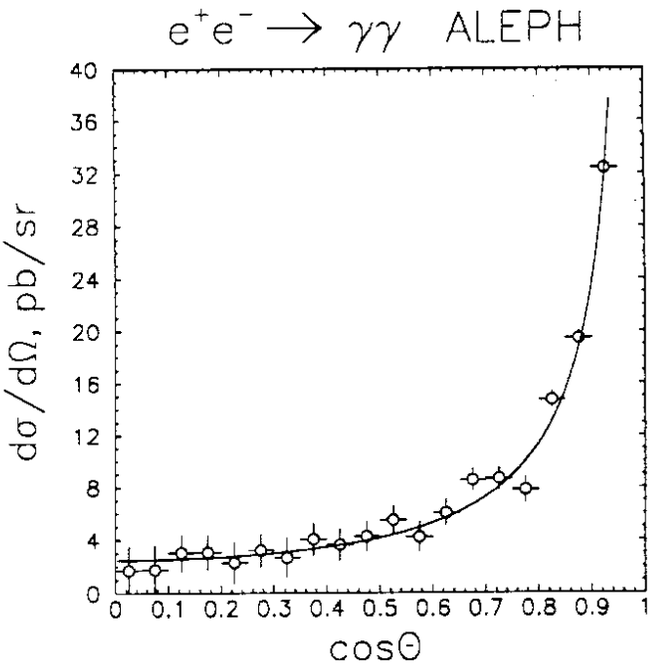

Figure 13: Differential cross section for the reaction $e^+e^- \to \gamma\gamma$ at the Born level. The data points are compared with the QED prediction at the effective energy = 91.225 GeV.

3.3 Contact term fits

Fits to the contact term models are performed by the maximum likelihood method, using the measured and predicted angular distributions expressed in terms of the number of events. The likelihood function has the form:

$$\mathcal{L} = g(n_0) \prod_{i=1}^{19} \mathcal{P}\left(N_i^{\mathrm{DATA}}\ ,\ N_i^{\mathrm{PRED}}(\Lambda)\right),$$

where $\mathcal{P}$ is the Poisson probability of observing $N_i^{\rm DATA}$ events while $N_i^{\rm PRED}$ are expected in the cosθ bin i. The error on the factor n_0, $\Delta n_o = 1.2\%$, includes all sources of systematic and statistical normalisation uncertainties.

The expected numbers of events in each cosθ bin is:

$$N_i^{\rm PRED}(\Lambda) = n_0 e_i \left(L\sigma_i^{\rm QED} a_i + \sum_{k=1}^{12} L_k \sigma_{ik}^{\rm CONTACT}(\Lambda) \right).$$

In this expression L is the total luminosity, $\sigma_i^{\rm QED}$ is the QED cross section at the Born level evaluated at $s = s_{eff}$ and the contact term contributions are summed over the 12 energies.

The $ee\gamma\gamma$ contact term amplitude is inversely proportional to the fourth power of Λ and thus the fit parameter ε is defined as

$$\varepsilon = (1/\Lambda)^4$$

for all models except for $L - R$, where $\varepsilon = (1/\Lambda)^8$.

3.4 Results of the contact term fits

The parameters ε and n_0 are determined for each model. All values of ε are compatible with 0 and those of n_0 with 1. The quality of the fits is estimated by the χ^2 test and the result is very similar to that for QED alone. One-sided 95% c.l. limits on the energy scale Λ and the resolving power are calculated from the formulae:

$$\Lambda^+ = \left(\varepsilon + 1.64\ \sigma^+\right)^{-1/4}, \qquad \Lambda^- = \left(-\varepsilon + 1.64\ \sigma^-\right)^{-1/4}, \qquad \lambda = (1.64\ \sigma)^{-1/4}.$$

For the $L - R$ model the power 1/4 has to be replaced by 1/8. When the value of Λ^+ or Λ^- exceeds λ, then it is bounded by λ. Table 7 summarises the results of the fits and the obtained limits.

	$\varepsilon^{+\sigma^+}_{-\sigma^-}$	λ (GeV)	Λ^+ (GeV)	Λ^- (GeV)
L, R	$(0.208^{+0.417}_{-0.430})10^{-8}$ GeV^{-4}	109	102	109
$L + R$	$(0.105^{+0.216}_{-0.214})10^{-8}$ GeV^{-4}	130	121	130
L - R	$(0.079^{+0.325}_{-0.303})10^{-15}$ GeV^{-8}	81	79	-
cut-off	$(0.107^{+0.225}_{-0.212})10^{-8}$ GeV^{-4}	129	120	129

Table 7: Results of fits of the $ee\gamma\gamma$ contact terms to the data. The values of ε are given with one standard deviation errors. λ is the resolving power and Λ^+ and Λ^- are the 95% c.l. limits on the energy scale Λ.

Fig. 14 shows the data and the maximum allowed contributions of the contact models L and $L - R$ plotted as a function of cosθ. The curves for the other two models are similar to those for the L model. For the $L - R$ model only one curve corresponding to Λ^+ is defined since the contact term contribution is always positive.

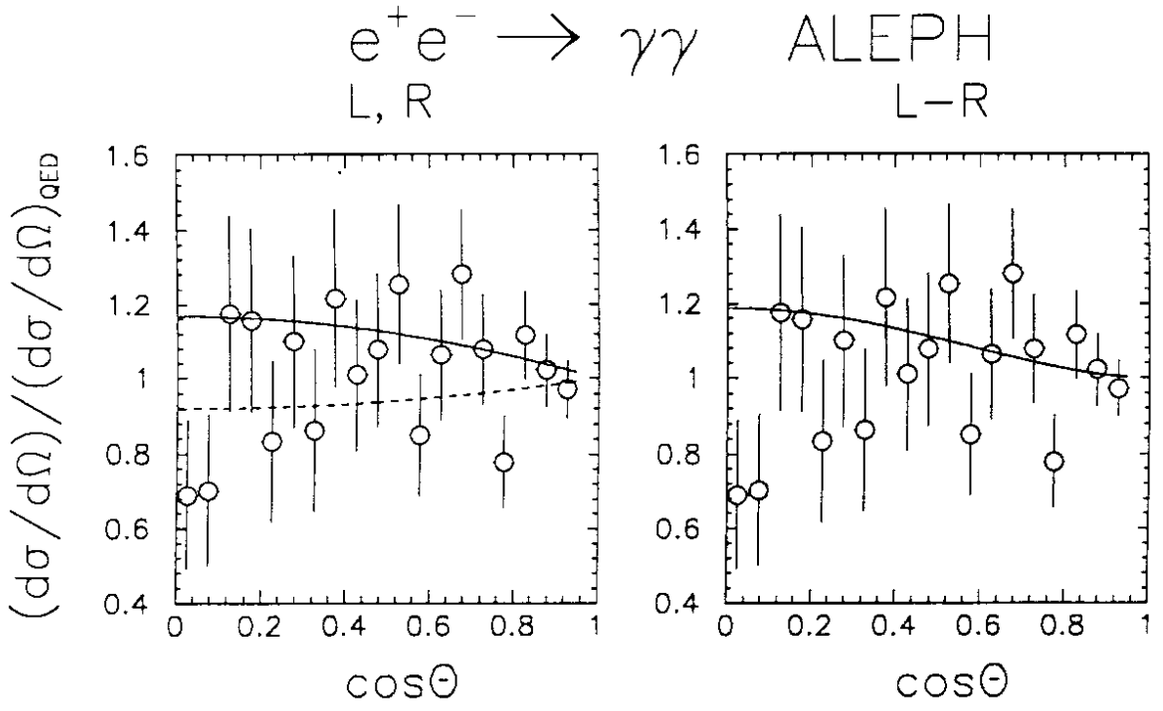

Figure 14: Results of the fits of contact models L, R, and $L-R$ for the reaction $e^+e^- \to \gamma\gamma$. The data points are the measured cross sections divided by QED predictions. The curves are the maximum allowed deviations at 95% c.l. corresponding to Λ^+ (continuous line) and Λ^- (dashed).

3.5 Comparison with lower energy data

The $ee\gamma\gamma$ contact term models L, R, $L+R$ and $L-R$ have been studied in e^+e^- interactions at TRISTAN at the total energy of about 56 GeV. Limits on the energy scale Λ were reported by three collaborations [24, 25, 26]. In order to combine these results, we assume that for each model and each experiment the errors on ε are symmetric and we deduce the value of ε and its error from the published values of Λ^+ and Λ^-. This could be done for the L, R and $L+R$ models but not for the $L-R$ model for which there is only one limit. The values of ε so obtained are then averaged over the three experiments and the overall limits on Λ from TRISTAN are calculated. They are compared with the ALEPH results in table 8 which shows also the best presently available limits on the energy scale of the $ee\gamma\gamma$ contact terms obtained by combining the results of TRISTAN and ALEPH. The condition $\Lambda < \lambda$ is imposed on all limits.

In spite of lower integrated luminosity, this analysis brings an improvement of the TRISTAN limits because LEP operates at higher energy. This behaviour is expected from the scaling law for the $ee\gamma\gamma$ contact terms

$$\Lambda^{\pm} \sim s^{3/8}\mathcal{L}^{1/8}$$

according to which the increase of energy is more rewarding than patience.

	L, R		$L+R$	
	Λ^+	Λ^-	Λ^+	Λ^-
TRISTAN	96	84	115	101
ALEPH	102	109	121	130
TRISTAN+ALEPH	114	111	135	132

Table 8: Limits at 95% c.l. on the energy scale Λ in GeV of the $ee\gamma\gamma$ contact terms from TRISTAN, ALEPH and both.

4 Conclusions

Searches for an indirect signal of a new interaction beyond the standard model have been carried out using differential cross sections for the reactions of lepton pair and photon pair production measured at several energies around the Z peak. No significant deviations from the standard model behaviour have been found.

Four-lepton contact term models assuming various chiralities of lepton currents are fitted to the data and lower limits on the energy scale Λ of a new interaction are set at 95% c.l. The limits vary in the range 0.9–4.7 TeV, depending on the model and on the lepton flavour. Lower energy results are improved, particularily for the reaction $e^+e^- \to e^+e^-$.

The present best limits deduced by combining ALEPH with PEP, PETRA and TRISTAN results are about 3 TeV for LL and RR, 3.5–4 TeV for RL and LR, and between 5 and 6 TeV for VV and AA models.

No evidence for deviations from QED is found in the reaction $e^+e^- \to \gamma\gamma(\gamma)$. A possible new interaction is parametrized by the $ee\gamma\gamma$ contact term models: L, R, $L+R$ and $L-R$. The values of the characteristic energy scale Λ are excluded by the ALEPH analysis up to 79–130 GeV depending on the model.

Acknowledgements

The authors are pleased to thank the SL Division at CERN for the operation of LEP. We gratefully acknowledge the support of the engineers and technicians in constructing and maintaining ALEPH. Those from us from non-member states wish to thank CERN for its hospitality.

References

[1] E. Eichten, K. Lane and M. Peskin, Phys. Rev. Lett. 50 (1983) 811.

[2] B. Schrempp, F. Schrempp, N. Wermes and D. Zeppenfeld, Nucl. Phys. B296 (1988) 1.
F. Schrempp, DESY 89-047 (1989)

[3] L.J. Hall and S.F. King, Nucl. Phys. B287 (1987) 551.

[4] P. Méry, M. Perrottet, F.M. Renard, Z. Phys. C38 (1988) 579.

[5] F. Boudjema and F. Renard, 'Compositeness', in 'Z Physics at LEP 1', (G. Altarelli, R. Kleiss and C. Verzegnassi, eds), CERN 89-08, vol 2 (1989) 1.

[6] ALEPH Collab., D. Decamp et al., Nucl. Instrum. Methods A294 (1990) 121.

[7] 'Update of Electroweak Parameters from Z Decays', ALEPH Collab., CERN/PPE 93-40, to be published in Phys. Lett. B.

[8] The LEP Collaborations: ALEPH, DELPHI, L3 and OPAL, Phys. Lett. B276 (1992) 247.

[9] F.A. Berends and W.L. Van Neerven, Nucl. Phys. B297 (1988) 429.

[10] W. Beenakker, F. Berends, S.C. van der Marck, Nucl. Phys. B349 (1991) 323.

[11] ALEPH Collab., D. Decamp et al., Z. Phys. C53 (1992) 1.

[12] ALEPH Collab., D. Decamp et al., Z. Phys. C53 (1992) 375.

[13] S. Jadach, B.F.L. Ward and Z. Wąs, Comput. Phys. Commun. 66 (1991) 276.
Computer program KORALZ, courtesy of S. Jadach, B.L.F. Ward and Z. Wąs.

[14] D. Bardin, W. Hollik, T. Riemann, Z. Phys. C49 (1991) 485.

[15] UA2 Collab., J. Alitti et al., Phys. Lett. B241 (1990) 150.
CDF Collab., F. Abe at al., Phys. Rev. Lett. 65 (1990) 2243.

[16] CDHS Collab., H. Abramowicz et al., Phys. Rev. Lett. 57 (1986) 298
and A. Blondel et al., Z. Phys. C45 (1990) 361.
CHARM Collab., J. V. Allaby et al., Phys. Lett. B177 (1986) 446
and Z. Phys. C36 (1987) 611.

[17] G. D'Agostini, Proceedings of the XXVth Rencontre de Moriond (1990), Editions Frontières, page 229.

[18] H. Kroha, Phys. Rev. D46 (1992) 58.

[19] CELLO Collab., H. J. Behrend at al., Z. Phys. C51 (1991) 149.

[20] S. D. Drell, Ann. of Phys. 4 (1958) 4.

[21] ALEPH Collab., D. Decamp et al., Physics Reports 216 (1992) 253.

[22] F. Berends and R. Kleiss, Nucl. Phys. B186 (1981) 22.

[23] F. Berends and R. Kleiss, Nucl. Phys B228 (1983) 537.

[24] AMY Collab., H. J. Kim et al., KEK preprint 89-52 (1989).

[25] TOPAZ Collab., K. Shimozawa et al., Phys. Lett B284 (1992) 144.

[26] VENUS Collab., K. Abe at al., Z. Phys. C45 (1989) 175.